Article

Not peer-reviewed version

Thermodynamic and Dynamic Transitions and Interaction Aspects in Reorientation Dynamics of Molecular Probe in Organic Compounds: A Series 1-Alkanols with TEMPO

Josef Bartoš * and Helena Švajdlenková

Posted Date: 28 August 2023

doi: 10.20944/preprints202308.1810.v1

Keywords: 1-alkanols; spin probe TEMPO; ESR; thermodynamic transitions; viscosity; crossover transition; polarity; proticity

Article

Thermodynamic and Dynamic Transitions and Interaction Aspects in Reorientation Dynamics of *Molecular Probe* in *Organic Compounds*: A Series *1-Alkanols* with *TEMPO*

Josef Bartoš [1,*] and Helena Švajdlenková [1,2]

[1] Polymer Institute of SAS, 845 41 Bratislava, Slovakia
[2] Department of Nuclear Chemistry, Faculty of Natural Sciences, Comenius University, 842 15 Bratislava, Slovakia; Helena.Svajdlenkova@savba.sk
* Correspondence: Jozef.Bartos@savba.sk

Abstract: The spectral and dynamic properties of *2,2,6,6-tetramethyl-1-piperidinyloxy (TEMPO)* in a series of *1-alkanols* ranging from *methanol* to *1-decanol* over a temperature range 100 K–300 K were investigated by *electron spin resonance (ESR)*. The main characteristic ESR temperatures connected with slow to fast motion regime transition, T_{50}'s and T_{X1}^{fast}'s are situated above the corresponding glass temperatures, T_g, and for the *shorter members* T_{50G}'s lie above or close to melting point, T_m, while the *longer ones* the $T_{50G} < T_m$ relationship indicates that the *TEMPO molecules* are in the local disordered regions of the *crystalline media*. The T_{50}'s and especially, T_{ini}^{fast}'s are compared with the dynamic crossover temperatures, $T_X^{VISC} = 8.72M^{0.66}$, as obtained by fitting the viscosity data in the liquid *n-alkanols* with the empirical power law. In particular, for $N_C > 6$ T_{X1}^{fast}'s lie rather close to T_X^{VISC} resembling *apolar n-alkanes* [PCCP 2018,*20*,11145-11151], while for $N_C < 6$ they are situated in the vicinity of T_m. The absence of a coincidence for lower*1- alkanols* indicates that the T_{50G} is significantly influenced by the mutual interaction between the *polar TEMPO* and the *protic polar medium* due to the increased polarity and proticity destroyed by the larger-scale melting transition.

Keywords: *1-alkanols*; *spin probe TEMPO*; ESR; thermodynamic transitions; viscosity; crossover transition; polarity; proticity

1. Introduction

In general, the dynamics of *glass-forming liquids*, i.e., *organics* and *inorganics* forming the supercooled *liquid* by their cooling below the melting temperature, T_m, and finished by a *liquid*-to-*glass* transition to a *glass* below the glass temperature, T_g, is non-monotoneous and exhibits a change at the so-called dynamic crossover temperature, $T_{cross} = T_B$ or T_X lying between T_m and T_g [1–12]. This dynamic crossover phenomenon between the relatively *weakly* and *strongly* changing supercooled *liquid dynamics* is observed using experimental techniques such as viscosity (VISC) at $T_{B,\eta}$ or T_X [1,2] and dielectric spectroscopy (DS) at $T_{B,DS}^{ST}$ [3,4] or $T_{B,DS}^{MG}$ [5] and $T_{B,DS}^{KWW}$ [6] as well as $T_{B,DS}^{SCH}$ [7]. Standardly, the crossover temperatures are determined by fitting the supercooled liquid dynamics using a combination of classic phenomenological expression for viscosity, η, or structural relaxation time, τ, such as the Vogel-Fulcher-Tamman-Hesse (VFTH) equation [1] or using the power law (PL) equation [2]. Lately, a special evaluation method via *Stickel's* temperature-derivative type of analysis or via more general *Martinez-Garcia's* apparent enthalpy analysis of the relevant dynamic quantities giving $T_{B,DS}^{ST}$ and $T_{B,DS}^{MG}$, respectively, were proposed [3–5]. Another ways of determination of the crossover temperature are based on the onset of increasing broadening of the frequency dispersion of the structural relaxation time distribution and on the change of structural relaxation strenght, $\Delta\varepsilon_\alpha$, leading to $T_{B,DS}^{KWW}$ or $T_{B,DS}^{SCH}$, respectively [6,7]. In the case of the PL eq. with T_X [2,9], this expression is rationalized theoretically within the idealized mode coupling theory (I-MCT) of liquid dynamics [11] by derivation of the same form of temperature dependence for viscosity and relaxation time with the so-called critical temperature, $T_c \approx T_X$.

Preprints (www.preprints.org) | NOT PEER-REVIEWED | Posted: 28 August 2023 doi:10.20944/preprints202308.1810.v1

The crossover transition is very significant feature of the supercoled liquid behavior as it is demonstrated by findings of several empirical correlations of T_B or T_X with various characteristic temperatures of a variety structural-dynamic phenomena, such as the decoupling or bifurcation of the primary α relaxation and the secondary β process, $T_{\alpha\beta}$, from DS or dynamic light scattering (DLS) [8]. Moreover, the crossover phenomenon is also reflected by various *extrinsic* probe techniques, such as FS, ESR and PALS. They revealed the decoupling of translation from rotation of *molecular probes* and the *medium* dynamics, at T_{decoup}, either for the relatively large *fluorescence probes* via fluorescence spectroscopy (FS) [13] or decoupling of rotation of the *spin probes* from the *medium* dynamics using electron spin resonance (ESR) [14]. Finally, crossover in the supercooled liquid state is also manifested by a bend effect in *ortho-positronium* lifetime τ_3 vs. T dependence as detected by positron annihilation lifetime (PALS). This slope change reflects a change in the free volume expansion at the characteristic PALS temperature T_{b1}^{L} above T_g in *amorphous glass-formers* [15]. Evidently, it is increasingly recognised that the dynamic crossover before glass transition temperature plays an essential if not fundamental role in our understanding glass transition phenomenon [9].

In contrast to the afore-mentioned cases of *amorphous glass-formers*, observations of the crossover transition in strongly crystallizing, i.e., relatively hardly supercooled *apolar* and *polar organics* is substantially more difficult. This is connected with the problem of formation of sufficiently large *amorphous* domains in the otherwise dominantly *ordered material* and subsequently, with their characterization by suitable *experimental technique*. Recently, we have proposed one *special method* of creation of such *amorphous* domains in *crystalline materials* consisting in an introduction of appropriate *molecular probe* disordering its immediate surroundings of the otherwise *ordered medium*. This included *spin probe* (*2,2,6,6-tetramethyl piperidin-1-yl)oxyl (TEMPO)* with V_{TEMPO}^{W} = 170 Å^3 in a series of *apolar n-alkanes* ranging from *n-hexane* to *n-nonadecane* using ESR technique [16]. On the basis of a close correlation between one of the characteristic ESR temperatures, namely, T_{X1}^{fast}, lying a bit above the main slow-to-fast transition at T_{50G} and marking the onset of pure fast motion regime of *TEMPO* and the crossover temperatures, T_X^{VISC}, as obtained from fittings the corresponding viscosity data for a series of *n-alkanes* using the PL eq., the dynamic crossovers in the local disordered regions around the *probe molecules* in the otherwise dominantly *crystalline organics* were detected.

One of the most important aspects of the extrinsic probe techniques, such as ESR is a potential interaction between the used *probe* and the *medium's constituents* which can in more or less extent influence the corresponding *probe* response from the investigated *organic matrix*. In our previous work on a series of *apolar* crystallizing *n-alkanes* we used one of the smallest *polar spin probe TEMPO* where this interaction aspect is supposed to be small [16]. The aim of this work is to test another types of *strongly* crystallizing *organic media* consisting of *protic polar compounds*, such as *1-alkanols* with a potential of the intermolecular *H*-bonding interaction not only between the own *polar molecules* but also between these *polar molecules* and *polar spin probe TEMPO*. The obtained spectral and dynamic data for the *TEMPO* on the family of aliphatic *monohydroxyalcohols* or *1-alkanols* $H(CH_2)_nOH$ with N_C = 1-10, i.e., ranging from *methanol* to *1-decanol* are interpreted using the newly analyzed viscosity data from the literature in order to reveal roles of the thermodynamic and dynamic transitions as well as of the interaction aspect in the main slow to fast transition behavior of the the used *spin probe TEMPO*.

2. Results and Discussion

2.1. Thermodynamic and crossover transition behaviors in 1-alkanols

It is well known that *1-alkanols* similarly as *n-alkanes* belong to the class of relatively easily crystalizing organic *compounds*. For this strong ordering tendency they require special ways of preparation of the *totally* or *partially amorphous samples* with one exception of *1-propanol* (*C3OH*) which is a very good *glass-former* [17].

2.1.1. Thermodynamic transitions in 1-alkanols

Figures 1 and 2 and Table 1 summarize the *literary* data about three basic thermodynamic transitions of *condensed materials*, i.e., *glass*-to-*liquid* (*devitrification*) transition of the *amorphous* phase

Preprints (www.preprints.org) | NOT PEER-REVIEWED | Posted: 28 August 2023 doi:10.20944/preprints202308.1810.v1

and *solid*-to-*liquid* (*melting*) transition of the *crystalline* phase to *liquid* one as well as *liquid*-to-*gas* (*evaporation*) transition of the *liquid* phase to *gas* one. In general, the corresponding transition temperatures, i.e., glass temperature T_g and melting temperature T_m for *1-alkanols* exhibit the *non-monotoneous* character as a function of their molecular size expressed by the number of carbon atoms in the chain, N_c, or molecular weight, M, while the boiling temperature, T_b, shows up the *monotoneous* type of dependence over the whole molecular size interval. In contrast to the *melting* with the well-defined T_m values [18], the T_g values measured so far exhibit a scatter up to 10 K which depend on both preparation procedure and measuring technique, such as dynamic-mechanical spectroscopy (DMS), differential thermal analysis (DTA) or differential scanning calorimetry (DSC) and dielectric spectroscopy (DS) [19–28], apparently diminishing with increasing molecular size. In spite of this fact, the T_g value for the shortest *1-alkanols* decreases from *methanol* (*C1OH*) to *ethanol* (*C2OH*) followed by *monotoneous* increasing trend starting from *C2OH* for DMS data [26] or from *1-propanol* (*C3OH*) for CAL ones [17]. As originally proposed by *Faucher & Koleske* [26], their DMS results could be described by the power law (PL)–type expression as a function of molecular weight M:

$$\boldsymbol{T_g} = \mathrm{A}\boldsymbol{M}^{\alpha} \tag{1}$$

where A, α are empirical parameters for a given homologous series of *compounds*. As seen from Figure 1A, they exhibit similar trend depending relatively strongly on the way of generation of *amorphous material* and the used set up in DMS or DTA, respectively. The latter values of T_g^{DTA} coinciding with T_g^{CAL} in cases of lower *1-alkanols*, such as *ethanol*, *1-propanol* and *1-butanol* studied by special CAL technique, i.e., quasiadiabatic calorimetry (QADC) [17,28] are considered to be more reliable ones mainly because of the experimental complexity of DMS.

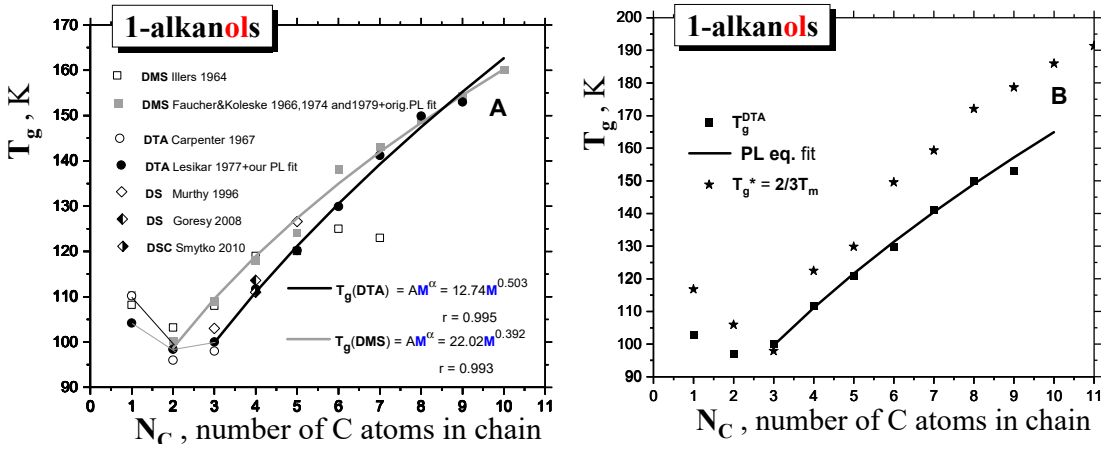

Figure 1. A.*Glass*-to-*liquid* temperature T_g of *1-alkanols* as a function of the molecular size expressed by the number of carbon atoms in the chain N_C. Two fits of the T_g's from DMS [20,26] and DTA data sets [22] via the PL equation of form: $T_g = AM^{\alpha}$ are included, B. Comparison of the T_g^{DTA} values with the empirical rule: $T_g^* = (2/3)\,T_m$.

As for the melting transition of ***1-alkanols***, the same expression can be approximately used for the melting points:

$$\boldsymbol{T_m} = \mathrm{C}\boldsymbol{M}^{\gamma} \tag{2}$$

where C = 8.41 and γ = 0.705 are empirical parameters for the melting of a given homologeous series of *compounds* as determined mainly from the calorimetric data [18]–Figure 2. Similar approach has been recently applied for *n-alkanes* and *monoalcohols* in spite of the very pronounced *zig-zag* effect for the *formers* with the similar γ value of 0.7 by *Novikov & Rössler* [29].

Finally, in Figure 1B the *estimated* values of glass transition, T_g^*, calculated according to the well-known empirical rule for many organic and inorganic glass formers: $T_g^* = (2/3)T_m$ [see e.g. Ref. 29–32] are also listed. From their comparison with the measured T_g data from DTA or DMS it follows that this rule is not valid for our series of the first ten *1-alkanols* with one exception for *C3OH*.

Preprints (www.preprints.org) | NOT PEER-REVIEWED | Posted: 28 August 2023 doi:10.20944/preprints202308.1810.v1

Alternatively, the measured T_m^{CAL}/T_g^{DTA} ratios fullfil rather another empirical rule of ~ 1.70 instead of T_m/T_g*= (3/2) = 1.50 valid again for *C3OH* only–Figure 3.

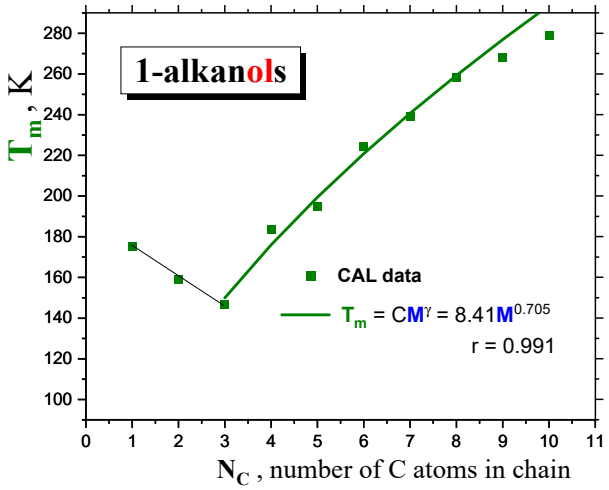

Figure 2. Melting temperature T_m of *1-alkanols* as a function of the molecular size expressed by the number of carbon atoms in the chain N_C. Fit of the T_m's from CAL data set from Ref.18 via the PL equation: $T_m = CM^{\gamma}$is included.

Table 1. Basic physical properties of investigated *1-alkanols*.

1-alkanol M	T_g	Tx^{VISC}	T_m[a]	T_b[a]	$A_{zz'}$(100K)[b]	A_{iso}(RT)[c]	μ_g[d]	μ[e]	ε_r(RT)[d]
g/mol	K	K	K	K	G	G	D	D	-
MeOH 32.04	108.2[f]	110.2[g]	135.8	175.2	338	37.87	16.46	1.70	2.70	33
103[h]	104.2[i]	135[2]								
EtOH 46.07	103.2[f]	100.2[g]	111	158.9	351	36.81	16.30	1.69	2.81	25.3
98.4[i]	96[j]	97[k]	111[5]	115[5]						
1-PrOH 60.10	108[f]	98[j]	109[g]	126.5	146.8	370.5	36.15	16.23	1.68	2.87	20.8
100[i]	103[l]	109.7[m]	139[9]							
1-BuOH 74.12	119[f]	111.7[i]	142	183.7	391	35.95	16.16	1.66	2.88	17.8
113.6[n]	111[o]	119[m]								
1-PentOH 88.15	120.1[f]	124[g]	168	194.8	411	35.90	16.05	1.70	2.97	15.1
120[i]	126.1[l]	127.4[m]								
1-HxOH 102.18	125[f]	138[g]	178	224.4	430	35.75	15.91	1.65	2.87	13.0
129.9[i]	135[m]									
1-HptOH 116.20	123[f]	143[g]	199.7	239	449	35.60	15.88	1.71	2.99	11.75
141.2[i]	141.9[m]									
1-OctOH 130.23	149[g]	149.9[i]	225.4	258.1	468	35.45	15.83	1.68	2.90	10.30
148.3[m]										
1-NoOH 144.25	153[i]	154.4[m]	236	268	487	35.25	15.75	1.60	2.73	8.83
1-DecOH 158.28	(160.1)[m]	239	279	501	35.15	15.70	1.60	2.70	7.93	

a.Ref.18; b.uncertainty = 0.05 G; c.uncertainty = 0.03 G; d.Ref.33; e.Ref.35; f.Ref.19; g.Ref.20; h.Ref.21; i.Ref.22; j.Ref.23; k.Ref.24; l.Ref.25; m.Ref.26; n.Ref.27; o.Ref.28.

Preprints (www.preprints.org) | NOT PEER-REVIEWED | Posted: 28 August 2023 doi:10.20944/preprints202308.1810.v1

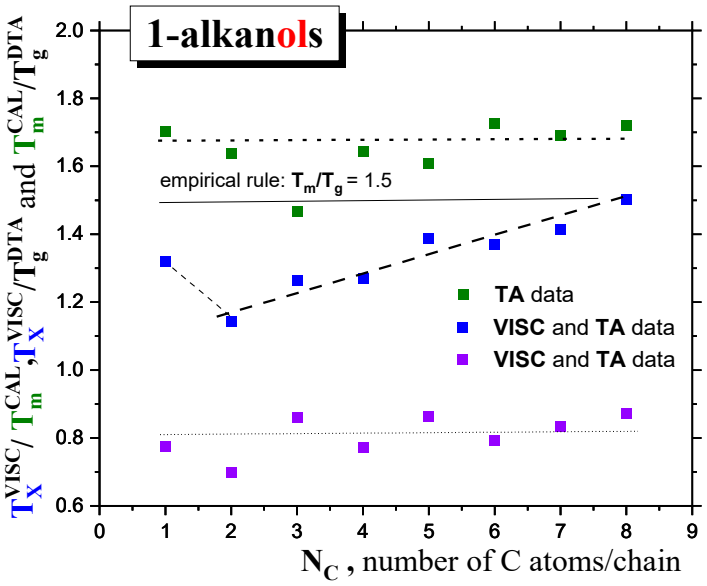

Figure 3. The T_m/T_g and T_X/T_g as well as T_m/T_X ratios of *1-alkanols* as a function of the molecular size expressed by the number of.

carbon atom in the chain N_C. In the case of T_m, the full horizontal lines represent the constant value of T_m/T_g = 1.5 from the empirical rule and dotted line with T_m/T_g ~ 1.68 for our series of *1-alkanols*, whereas in the case T_X with one exception for *C1OH* increasing linear trend of T_X/T_g is found. Finally, T_X/T_m ~ 0.81.

2.1.2. Dynamic crossovers in 1-alkanols

As mentioned in Introduction, the crossover temperature in the supercooled liquid state of many organic *compounds* can be obtained using the power law (PL) equation connecting the viscosity of liquids, η, with temperature T in the *normal* liquid and *weakly* supercooled liquid states [2,9,16]. Figures 4 and 5 and Table 1 as well as Figure 6 give the results of such a way of determination of the crossover temperature, T_X. Thus, Figure 4 presents compilations of the viscosity data for a series of ten *1-alkanols* ranging from *methanol* (*C1OH*) up to *1-decanol* (*C10OH*) as a function of temperature mostly from the two large summarizing literature sources [33,34]. Most of the viscosity data of *1-alkanols* falls into the *normal* liquid state between the melting temperature, T_m, and the boiling temperature, T_b. For two lower *members* of this series, namely, *ethanol* (*C2OH*) and *1-propanol (C3OH)*, the viscosities were also measured in the supercooled liquid state *below* the corresponding T_m's; sligthly for the *former* [36] but even almost down to the corresponding T_g for the *latter* because of its very good glass-forming ability [36–38]. All the viscosity data for a serie of the first ten *1-alkanols* can be described by the power law (PL) equation:

$$\eta\,(T) = \eta_\infty \left[\frac{(T - T_X)}{T_X}\right]^{-\mu} \tag{3}$$

where, η_∞ is the pre-exponential factor, T_X is the empirical characteristic dynamic PL temperature or the theoretical critical MCT temperature T_c and μ is a non-universal coefficient. The corresponding fitting curves are plotted in Figure 4 and the obtained crossover temperatures T_X are listed in Table 1 and Figure 6. In the afore-mentioned case of *1-alkanols* for which the viscosity data also in the supercooled liquid state exist [43], the extracted T_X's for, e.g., *C2OH* from fitting over the usual *normal* liquid state range T_b - T_m = 192 K and over the whole accessible temperature range of 227 K [36] = T_b –T_{min} = 227 K, change by 4 K only. Similarly, for very good *glass-former C3OH* this difference reaches

Preprints (www.preprints.org) | NOT PEER-REVIEWED | Posted: 28 August 2023 doi:10.20944/preprints202308.1810.v1

3 K towards the lower value by including also the *strongly* supercooled liquid range data from Ref. 36 - see Figures 5A,B. Thus, the PL equation. fit over the *normal* liquid state only appears to be a very good approximation to obtain the T_X's lying in the supercooled liquid state below the corresponding T_m's in *strongly* crystallizing organics, such as *1-alkanols*. These are also listed in Table 1 together with scarce determinations on the first three *members*, namely, *C1OH, C2OH* and *C3OH* by other *authors* [2,5,9].

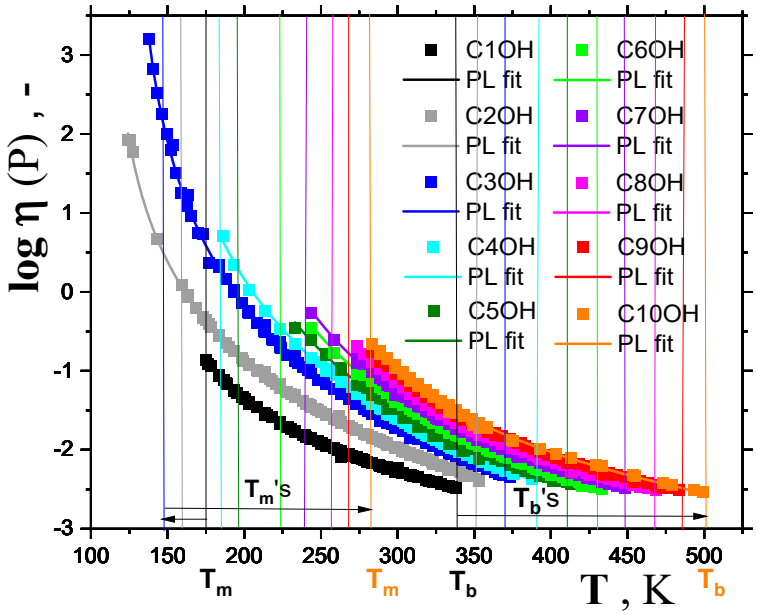

Figure 4. Viscosities for a series of *1-alkanols* as a function of temperature together with the respective power law (PL) equation (3) fits. The vertical lines in the same colors as the corresponding experimental points for each *member* of a series of *1-alkanols* mark the melting temperatures (on left) and the boiling points (on right) with two extrema demonstrations for *methanol* (black points and lines) and *1-decanol* (orange points and lines).Trends in T_m's and T_b's show two arrows at bottom of the plot.

Preprints (www.preprints.org) | NOT PEER-REVIEWED | Posted: 28 August 2023 doi:10.20944/preprints202308.1810.v1

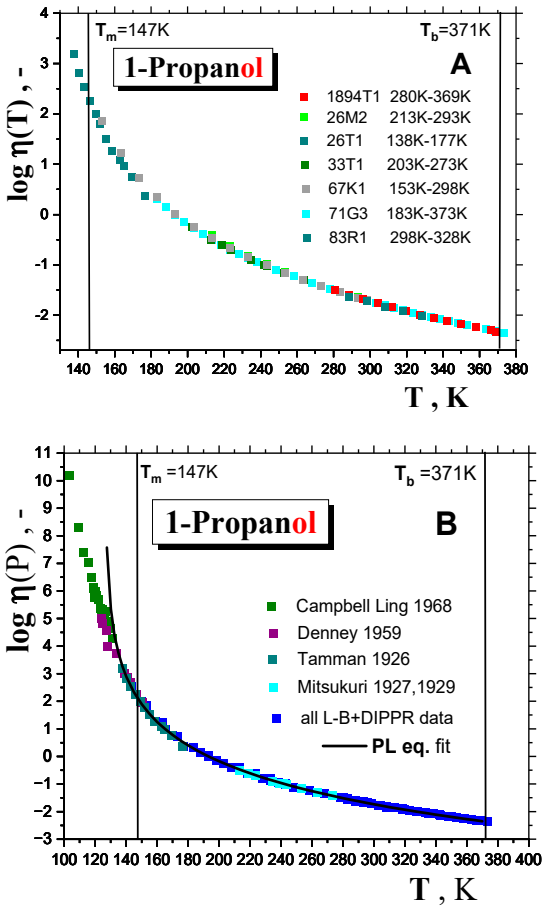

Figure 5. Viscosity of a good *glass-former 1-propanol* over (A) restricted temperature range from T_b down to sligtly below T_m using the data sets summared in Refs.33 (Landolt-Börnstein Table data) and Ref. 34 (DIPPR data) and (B) an extraordinary wide temperature range from T_b down almost to T_g with the additionally included data from Refs.36-38 in the *strongly* supercooled liquid state as well as from Ref.39 in the liquid one together with the best PL equation fit.The original references marked such as 1891T1, 26M2,.can be found in Ref.33.

It is shown that the PL equation is valid for a large number of *organic molecular glass formers* over rather higher temperature range [2,5,9] It is also known, the I-MCT works very well also for the relatively lower viscosity regime [11]. In reality, although the viscosity does not diverge at $T_X \approx T_c$, several analyses of the slightly supercooled and normal liquid dynamics in various *organic glass formers* in terms of the extended mode coupling theory (E-MCT) which removes this singularity, provide the *same* crossover temperature in the supercooled liquid phase [11,40]. Thus, the T_X parameter marks two distinct regimes of the *strongly* and *weakly* supercooled liquid dynamics [11]. In particular, it corresponds to the onset of dynamic heterogeneities, i.e., regions with slower dynamics embedded into regions of higher dynamics, when the decoupling of translation from rotation of the *molecular tracers* and the decoupling of rotation of the *molecular tracer* from that of the *medium constituents* occur and the classic Stokes-Einstein law or Debye-Stokes-Einstein law, respectively, are violated [9,14].

Figure 6. displays the molecular size dependence of the *extracted* dynamic crossover temperature T_X for *1-alkanols* together with its fitting curve of a similar form as for T_g and T_m. Similarly to the T_g and T_m quantities, after the initial decrease to the second lowest *member* the series of nine *1-alkanols* follows the power law formula:

$$\boldsymbol{T_X} = \mathrm{B}\boldsymbol{M}^{\beta} \tag{4}$$

Preprints (www.preprints.org) | NOT PEER-REVIEWED | Posted: 28 August 2023 doi:10.20944/preprints202308.1810.v1

with the β exponent equals 0.656 lying in between those for the glass temperature, T_g(α = 0.503) and melting point, T_m (γ = 0.705).

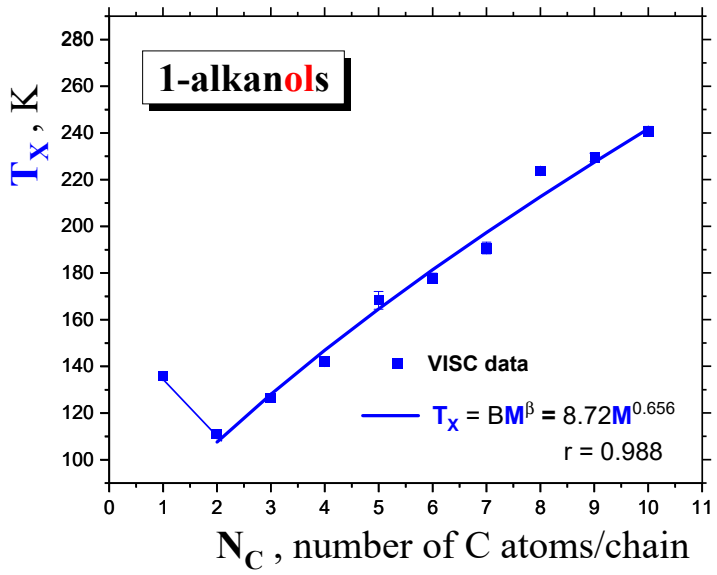

Figure 6. Dynamic crossover temperature T_X of *1-alkanols* as a function of the molecular size expressed by the number of carbon atoms in the chain N_C. Fit of the T_X's from VISC data via the PL equation of form: $T_X = BM^{\beta}$ is included.

Finally, returning to Figure 3, a comparison of T_X/T_g vs. T_m/T_g dependencies as a function of molecular mass *M* starting from *C2OH* shows *diametrally* different trend for the former quantity with respect to the latter one, i.e., increasing distance of the particular T_X from the respective T_g with the increasing molecular size of *1-alkanol*. This finding together with the almost same relative distance of T_X from T_m being ca. 0.81xT_m indicates that the larger *molecule* of *1-alkanol* the larger temperature range of the existence of the *strongly* (or *deeply)* and correspondingly the shorter *weakly* (*slightly*) supercooled liquid state. On the other hand, on cooling of the smaller *1-alkanols*, the *weakly* supercooled liquid state persists for longer *T* range with the correspondingly shorter *deeply* supercooled liquid range.

2.2. ESR data

2.2.1. General spectral and dynamic features

Figure 7 presents the $2A_{zz'}$ vs. *T* dependencies for our series of the *spin systems: TEMPO/1-alkanols*. In all cases, a quasi-sigmoidal courses of these plots are found with the higher $2A_{zz'}$ values in a slow motion regime at relatively lower temperatures and the lower $2A_{zz'}$ ones in a fast motion one in relatively higher temperature region.The main feature of $2A_{zz'}$ vs. *T* dependencies is a more or less *sharp* change at the main characteristic ESR temperature T_{50G}, at which the $2A_{zz'}(T_{50G})$ value reaches just 50 Gauss corresponding to the correlation time of the *TEMPO* in a typical *organic medium* around a few ns. Note that the detailed spectral simulations of the *TEMPO* dynamics in several *organics*, including one of the investigated *1-alkanols*, namely, *1-propanol* [41], revealed that the *spin probe* population even at T_{50G} is not completely in the *fast* motion regime which occurs at a bit higher temperature T_{X1}^{fast}. In addition to these main characteristic ESR temperatures T_{50G} and T_{X1}^{fast} other effects appear at T_{X1}^{slow},T_{X2}^{fast} a discussion of which goes beyond the scope of this work and therefore it will addressed elsewhere. All the $2A_{zz'}$ vs. *T* plots include also the afore-mentioned thermodynamic and dynamic temperatures: T_g, T_m or T_X, respectively. Then the mutual relationships of these three basic characteristic thermodynamic and dynamic temperatures to T_{50G} and T_{X1}^{fast} in a series of *1-alkanols* will be discussed below in Section 2.2.2.

Preprints (www.preprints.org) | NOT PEER-REVIEWED | Posted: 28 August 2023 doi:10.20944/preprints202308.1810.v1

In principle, the main slow-to-fast motion transition of the *TEMPO* in any *organics* is related not only to these thermodynamic and dynamic transitions but it may also be influenced by further factors, such a potential mutual interaction of a *polar spin probe* with *organic media*, especially, *polar ones*. The values of anisotropic hyperfine constants $A_{zz'}$(100 K) at the lowest measured temperature of 100 K and of isotropic ones A_{iso}(RT) at room temperature are summarized in Table 1. Their dependencies on N_C as well as on some relevant *bulk* property of *media* such as *bulk* polarity of *media* through their dielectric constant, ε_r, will be discussed in the Sect.2.2.3.

Finally, the mutual connection between temperature parameters of the slow-to-fast transition and the thermodynamic as well as dynamic ones in relation to the polarisation interaction of the *polar TEMPO probe* with a series of *polar 1-alkanols* are discussed in Sect.2.2.4.

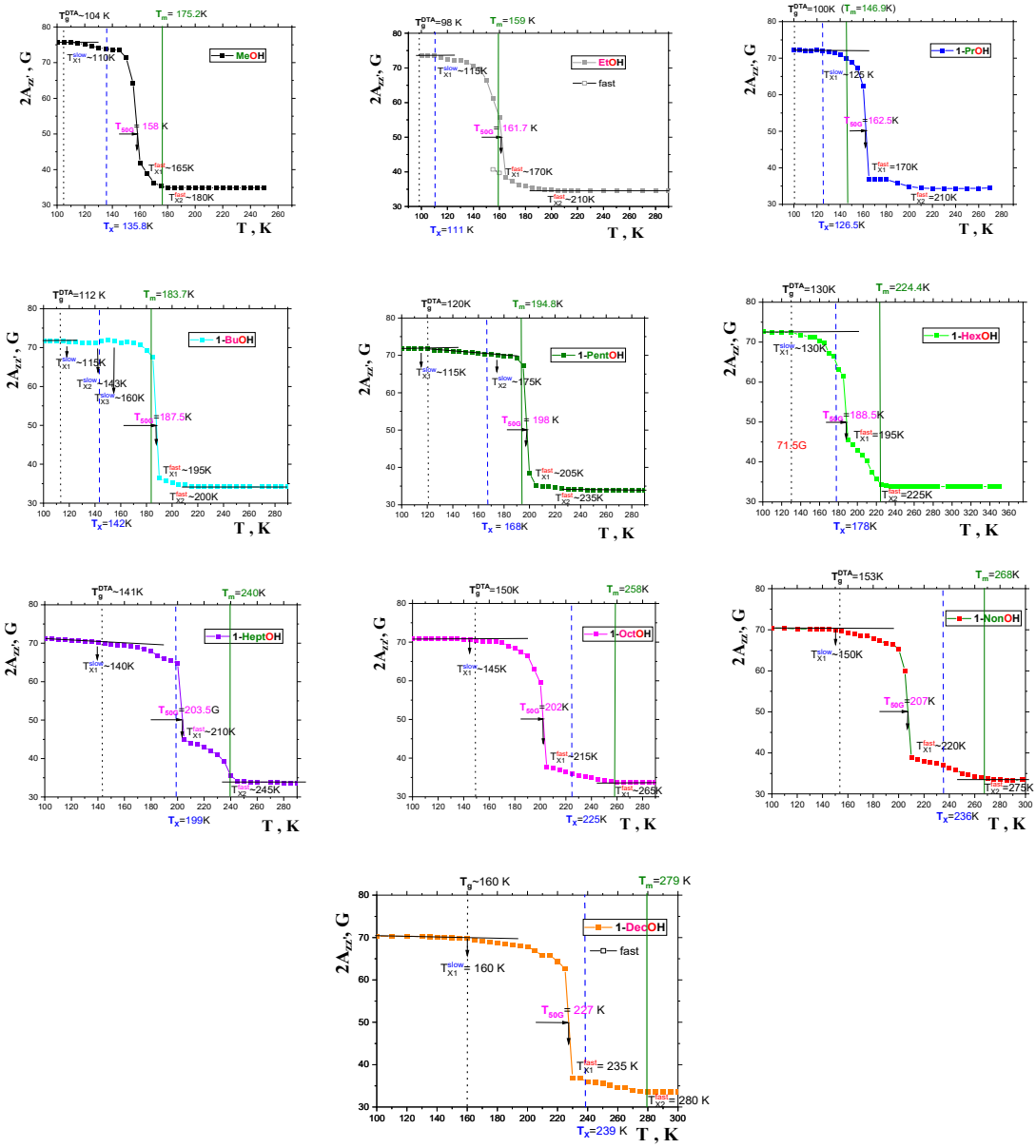

Figure 7. Spectral parameter $2A_{zz'}$ for a series of *1-alkanols* as a function of temperature. The characteristic ESR temperatures T_{Xi}^{slow}, T_{50G} and T_{Xi}^{fast} are marked and their mutual relationships with the thermodynamic temperatures T_g^{DTA} and T_m and dynamic one T_X depicted by black, olive and blue color lines are discussed in the text in detail.

Preprints (www.preprints.org) | NOT PEER-REVIEWED | Posted: 28 August 2023 doi:10.20944/preprints202308.1810.v1

2.2.2. The mutual relationships of T_{50G} and T_{X1}^{fast} with thermodynamic and dynamic transitions

In Figure 8 global comparisons of the characteristic ESR temperatures T_{50G} and T_{X1}^{fast} with the afore-mentioned thermodynamic and dynamic temperatures T_g, T_X and T_m are presented. In all the cases, the slow-to-fast transition in all *1-alkanols* occur above the corresponding *glass*-to-*liquid* transition T_g's, i.e., in the amorphous phase *liquid sample* or in the *local* amorphous *liquid* zones of *partially crystalline matrices,* at least. Figure 9 expresses these comparisons in terms of the corresponding ratios: T_{50G}/T_m, T_{50G}/T_X and T_{X1}^{fast}/T_m, T_{X1}^{fast}/T_X. We can approximately distinguish two distinct regions of these ratios with a boundary at around *C5OH*:

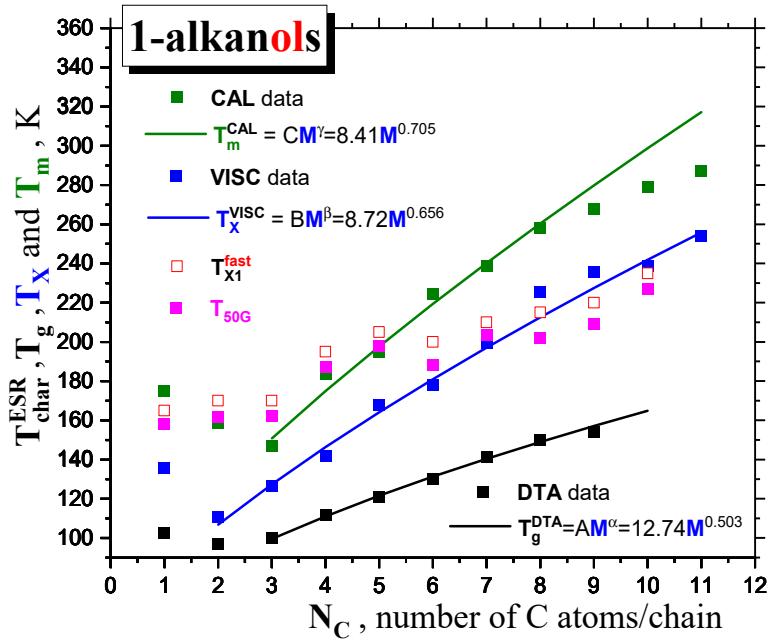

Figure 8. Comparison of the characteristic ESR temperatures T_{50G} and T_{X1}^{fast} with the thermodynamic and dynamic temperatures T_g^{DTA}, T_X and T_m together with their corresponding PL fits.

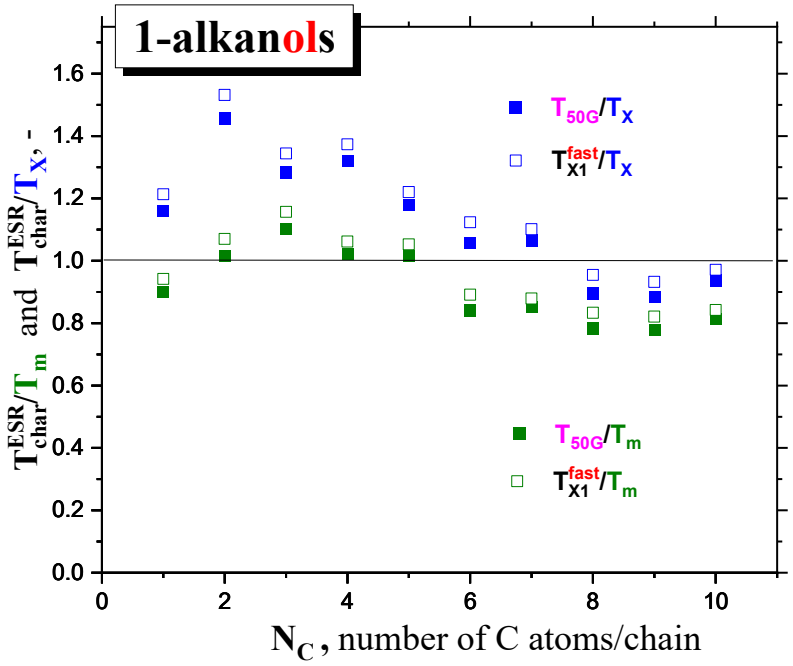

Figure 9. Comparison of the ratios of the characteristic ESR temperatures T_{50G} and T_{X1}^{fast} with the dynamic and thermodynamic temperatures T_X or T_m, respectively.

Preprints (www.preprints.org) | NOT PEER-REVIEWED | Posted: 28 August 2023 doi:10.20944/preprints202308.1810.v1

low ***M*** region: ***C1OH-C5OH*** with $T_{50G}/T_m \approx 1$ (5)

high ***M*** region: ***C6OH-C10OH*** with $T_{50G}/Tx \approx 1$ (6)

So, for higher *members* starting at *C6OH* to *C10OH* with a relatively longer aliphatic part we observe a quite plausible closeness between the characteristic ESR temperatures and the *Tx*'s indicating that the main ESR transition is related to the dynamic crossover between the *deeply* and *slightly supercooled liquid* state. This basic finding is similar to the previous one for a series of *n-alkanes* [16] with the fact that the *Tx*'s for *n-alkanols* are higher than the *Tx*' ones for the corresponding *n-alkanes* with the same number of *C atoms* in the *molecule*. This difference indicates that the *spin probe TEMPO* is not fully surrounded by the *apolar aliphatic parts* of the *n-alkanol molecules* and that the *polar -OH groups* influence its dynamics as it will be discussed later in Section 2.2.3. Anyway this indicates that the immediate environment of the molecular-sized *spin probe TEMPO* is locally disordered and subsequently, sensitive to the crossover transition in this *local* amorphous phase. On the other hand, for low *M members* from *C1OH* to *C5OH* T_{50G} and T_{X1}^{fast} lie significantly above the corresponding *Tx* values and they are situated rather in the vicinity of the corresponding melting temperatures, T_m. This indicates that the slow- to-fast transition of *TEMPO* appears to be related to the global disordering process connected with the *solid*–to-*liquid* state phase transition in the otherwise *partially crystallized samples.*

2.2.3. Isotropic and anisotropic hyperfine constants A_{iso}(RT), $A_{zz'}$(100 K) as a function of N_C and polarity and proticity of 1-alkanols

Figure 10. displays the anisotropic hyperfine constant, $A_{zz'}$(100K) and the isotropic. hyperfine constant, A_{iso}(RT), of the *TEMPO* as a function of the chain length in a series of *1-alkanols* studied. Our values of A_{iso}(RT) for *TEMPO* are quite consistent with the scarce ones obtained for lower *members* of our series, namely, *C1OH-C4OH* [42–44]. Although both the quantities are decreasing with increasing chain size, a significant difference does exist in the corresponding trends. The former quantity has two clearly regions of distinct behavior: a sharper decreasing trend for low-*M members* and the weaker one for higher-*M ones* above N_C ~ 4. On the other hand, the A_{iso}(RT) parameter shows up rather slighter reduction with the number of C atoms in the molecule, N_C.

These basic empirical findings can be discussed in relation to polarity of a set of the *polar media* with the dissolved *polar spin probe TEMPO* μ_{TEMPO} ~ 3D [45] from both the phenomenological and theoretical viewpoints. First, the A_{iso}(RT) values can be related to various measures of polarity of the *medium*, e.g., the dipole moment of the *medium's molecule*, $\mu_{entity,X}$, as a measure of the polarity of *individual entity* in a given phase state X = g,l or the static dielectric constant of the *medium*, ε_r(RT), as a measure of the polarity of the *bulk* liquid *medium* as listed in Table 1. In the first case evidently no any relationship does exist due to the quasi-constant values of the *gas*-phase μ_g = 1.66±0.05 D or the *liquid*-phase μ_l = 2.84 ± 0.15 D dipole moments [34,35]. On the other hand, Figure 11 displays the mutual relationship between the isotropic hyperfine constant, A_{iso}(RT), and the dielectric constant, ε_r(RT), of *1-alkanols* [34] together with of the latter quantity at RT as a function of the number of C atoms in chain in insert. Both the quantities decrease with N_C resulting into A_{iso} (RT) vs. ε_r (RT) relationship with approximately two regions of a distinct behavior: i) for lower *polar 1-alkanols* (*C10OH-C5OH*) with ε_r < ~ 17 with a strong sensitivity of A_{iso}(RT) to polarity and a weak one to proticity and ii) for higher *polar 1-alkanols* (*C3OH-C1OH*) with ε_r > ~ 17 with weak sensitivity of A_{iso}(RT) to polarity and stronger to proticity due to the increased population of *HO-groups* potentially interacting with the *spin probe TEMPO molecule*. The apparent boundary between both regions occurs at N_C = 4-5, i.e., for *1-butanol* or *1-pentanol*, where the ε_r(RT) vs. N_C(RT) plot changes rather pronouncedly from the *sharply* decreasing dependence to the *slightly* decreasing one and where, at the same time, conformational degrees of freedom and related enhanced alignement of the *apolar* parts of the molecules start to occur. Interestingly, in spite of the absence of ε_r(100K) data for their *direct* comparison with $A_{zz'}$(100K), the boundary for this quantity seems to be consistent with that for A_{iso}(RT) suggesting a significant role of polarity and proticity in both the mobility states of the *spin*

Preprints (www.preprints.org) | NOT PEER-REVIEWED | Posted: 28 August 2023 doi:10.20944/preprints202308.1810.v1

probe TEMPO. These findings of a solvent dependence of the different ESR parameters are consistent with the previous ones for A_{iso}(RT) [46,47] as well as for $A_{zz'}$(77 K) [48,49].

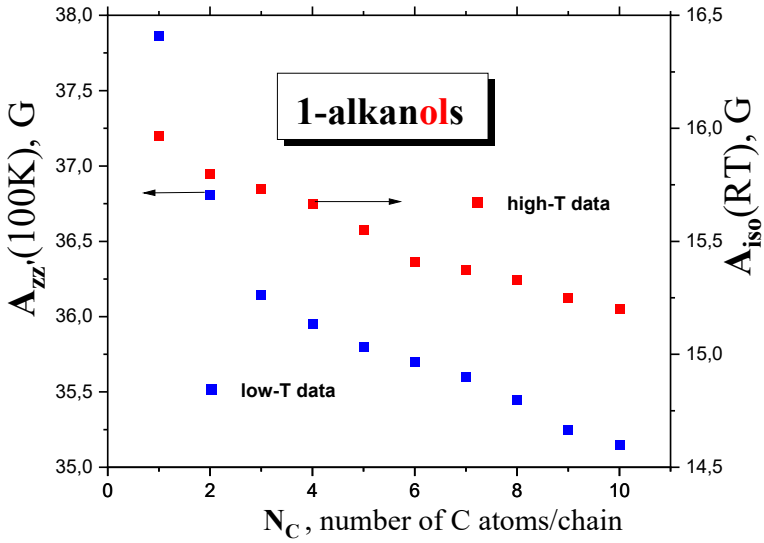

Figure 10. Hyperfine constants of *TEMPO* $A_{zz'}$(100 K) and A_{iso}(RT) in a series of ten *1-alkanols* as a function of N_C.

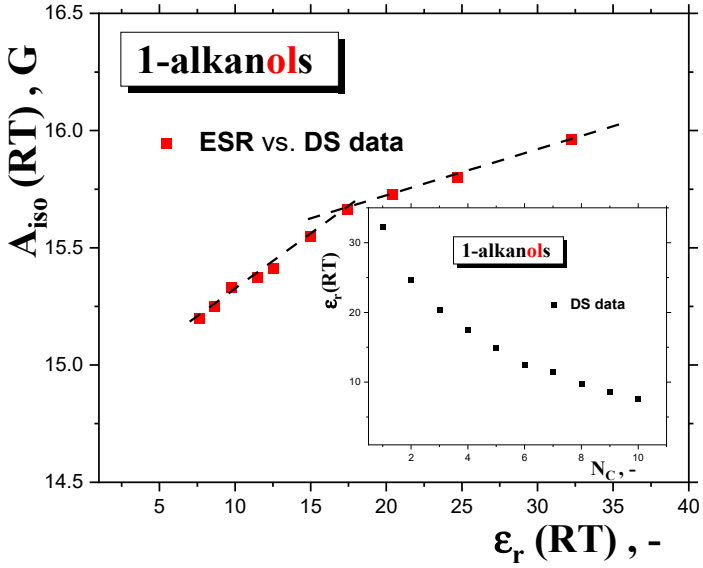

Figure 11. Empirical relationship between the isotropic hyperfine constant, A_{iso}(RT), and the relative permitivity, ε_r(RT), of *1-alkanols*. Insert contains the latter quantity at RT from Table 1 as a function of the number of C atoms in chain.

This our basic finding is similar to that for another larger nitroxide spin probe 1-oxyl- 2,2,5,5-tetramethyl pyrroline-3-methyl)methanethiosulfonate (MTSSL) in a series of 17 solvents ranging from apolar methylbenzene (toluene) [ε_r(RT) = 2.4] to highly polar water [ε_r(RT) = 80.4] and even more polar formamid [ε_r(RT) = 109] including most of the members of our 1-alkanol series with one expection for 1-pentanol [50]. These authors similarly distinguished the following two regions, i.e., „apolar" region for ε_r(RT) < 25, where the sensitivity of A_{iso}(RT) and $A_{zz'}$(77K) to the polarity expressed

Preprints (www.preprints.org) | NOT PEER-REVIEWED | Posted: 28 August 2023 doi:10.20944/preprints202308.1810.v1

by ε_r(RT) is large and „polar“ region for ε_r(RT) > 25, where the sensitivity of A_{iso}(RT) and $A_{zz'}$(77 K) to the polarity is small and the change is ascribed to the medium proticity.

However, it is evident that this their dividing is rather arbitrary and very rough because the former „*apolar*“ region include also many of our *polar 1-alkanols*. In connection with the afore-mention empirical relation between spectral parameters and *bulk* polarity, more elaborate theoretical approaches based on models of the *medium* as a dielectric *continuum* with dielectric constant, ε_r, and the *molecular solute*, e.g., *polar spin probe* as a molecular entity localized in a *spherical* cavity [47,51] can be discussed. Within the reaction field concept of the polarization of the *continuum medium* by the *polar solute*, one obtains for the *Onsager's* reaction field [52] and *Böttcher's* reaction field [53] the following functional relations: $A_{iso} = f[(\varepsilon_r-1)/(\varepsilon_r + 1)]$ [47] or $A_{iso} = f[(2\varepsilon_r + 1)/(2\varepsilon_r + n_D^2)]$, where n_D is the refraction index of the pure *nitroxide* [51], respectively. Figure 12 displays test of the validity of the first functional dependence for two basic groups of *organic compounds* at *RT* doped by *TEMPO*. The first is represented by a series of *apolar* and *aprotic polar solvents* which range from *apolar benzene (BZ)* with ε_r(RT) = 2.3 to highly *polar* but *aprotic dimethylsulphoxide (DMSO)* with ε_r(RT) = 48.9 as taken from Ref.50. The other group including our series of ten *1-alkanols* from *methanol* with ε_r(RT) = 33 to *1-decanol* with ε_r(RT) = 7.9 differs significantly from the predicted linear trend due to the specific *protic* character of the *molecules* allowing for the *H*-bond formation between the *polar spin probe TEMPO molecule* and the *alkanol's one(s)*. This is quite consistent with the maximal value of A_{iso} (RT) = 17 Gauss [44] for highly *polar* and *protic water* ε_r(RT) = 80.4 [50]. The relative large difference between *water* and the first *member of alkanol family* is on the basis of theoretical calculations using density functional theory (DFT) interpreted in terms of the complexation of *nitroxide* with two *water* or one *methanol molecules*, respectively [45,50]. Moreover, a closer inspection of this group of *protic polar compounds* confirms a distinguishing a series of *1-alkanols* into two subgroups with the distinct slopes of A_{iso}(RT) as a function of the corresponding dielectric function: i) weaker for the higher *members* from *C10OH* to *C6OH* and ii) stronger for the shorter ones from *C5OH* to *C1OH* with the approximate boundary between *C5OH* and *C6OH*, i.e., for ε_r(RT) ~ 16.5. Similar situation can be found for the *Böttcher* type of reaction field due to a linearity between the respective functional forms. Both these findings appear to be consistent with the purely empirically found boundary at *C4OH - C5OH* as seen from the A_{iso}(RT) vs. ε_r(RT) plot *without* inclusion of the polarization interaction between the *polar solute* and the *solvent* in Figure 11.

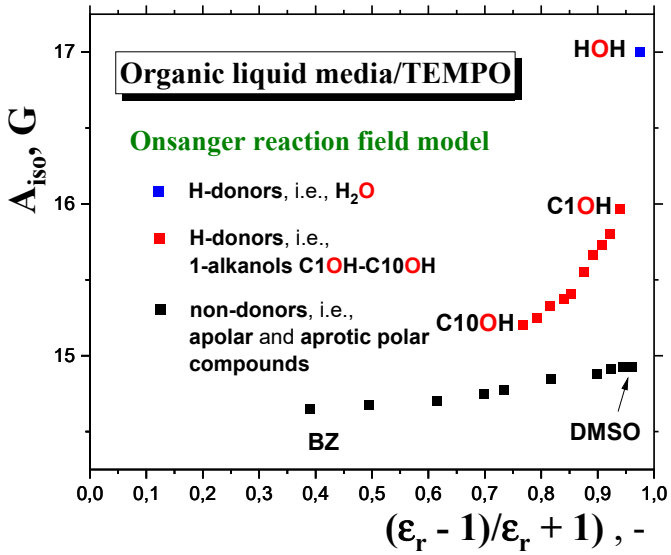

Figure 12. Test of the Griffith - Onsanger model for isotropic hyperfine constant, A_{iso}(RT) as a function of polarization expression [ε_r(RT)-1]/[ε_r (RT)+1] of the Onsanger reaction field model for three types of media: *apolar*, such as *benzene (BZ)* [44] and *aprotic polar*, such as *dimethylsulphoxide (DMSO)* [44] and *protic polar* compounds such as *water* [44] and our series of ten *1-alkanols*.

Preprints (www.preprints.org) | NOT PEER-REVIEWED | Posted: 28 August 2023 doi:10.20944/preprints202308.1810.v1

2.2.4. Connection of the main slow to fast motion transition of the spin probe TEMPO with the polarity and proticity and the thermodynamic and dynamic transition behavior of 1-alkanols.

In Figures 8 and 9 in Section 2.2.2 we have compared the characteristic ESR temperatures T_{50G} and T_{ini}^{fast} of the slow to fast transition of *TEMPO* in a series of *1-alkanols* with the dynamic crossover T_X and thermodynamic transition temperatures T_m, and their mutual ratios as a function of molecular size, N_C, of the *media*. In particular, we revealed rather a *step*-like change in the main *spin probe TEMPO* transition from that related by dynamic crossovers at around T_X for the longer *chains* to that related to thermodynamic transitions around T_m for the shorter *molecules* at N_C ~ 5.

Next, in Figures 10, 11 and 12 in Section 2.2.3 we presented the relations of spectral parameters A_{iso}(RT) and $A_{zz'}$(100 K) to N_C as well as their phenomenological and theoretical relationships of especially A_{iso}(RT) to polarity properties for a set of *1-alkanols*. Here, we observed a change in the trend of hyperfine interactions with polarity and proticity of *1-alkanol media* at N_C ~ 4. Now, a combination of these findings indicates that the slow to fast transition in mobility of *TEMPO* in a series of *1-alkanols* is relatively strongly dependent on the strenght of intermolecular interactions between the *polar* constituents of the *polar media* as well as between the *polar spin probe* and the polarity and proticity of the *1-alkanols* investigated. In the longer *members* of the *1-alkanol family* with the relatively higher population of the *apolar* aliphatic *methylene groups* related to a weakly changing polarity, the slow to fast transition is related mainly to the dynamic crossover process around T_X similarly as in the *apolar n-alkanes* [16]. On the other hand, in the shorter *members* with the relatively higher dielectric constants and proticity due to the relatively higher population of the *polar hydroxyl groups*, the larger-scale disorder process connected with the *solid*-to-*liquid* phase transition around T_m is needed for destroying not only the dense *H*-bonding *network* between the *medium'd molecules*, but also of clusters of the *polar TEMPO molecules* with them and subsequently, to the appearance of slow-to-fast transition in mobility of *TEMPO*. The critical molecular size of *1-alkanol* for this *step*-like change in the slow to fast transition of *TEMPO* lies at N_C ~ 5 below which the polarity and proticity aspects of the *media* become to be dominanting factors.

3. Experimental

3.1. Materials and Methods

A series of *1-alkanols* ranging from *methanol* to *1-decanol* from Sigma-Aldrich, Inc was used as model *protic polar media*. The reason for our choice of this series stems from the fact that all of the used *1-alkanols* are in the liquid state at room temperature because of easy *spin probe system* preparation. As an *extrinsic* particle, the *spin probe 2,2,6,6-tetramethyl-1-piperidinyloxy (TEMPO)* of the *quasi-spherical* shape and the relative high dipole moment of μ_{TEMPO} = 3 D [45] was applied in the *deoxygenated 1-alkanols* with a very low concentration of ~ $5x10^{-4}$ M.

3.2. ESR

ESR measurements of the very dilute *spin systems 1-alkanol/TEMPO* were performed on the X-band Bruker–ER 200 SRL spectrometer operating at 9.4 GHz with a Bruker BVT 100 temperature variation controller unit. ESR spectra were recorded after cooling with a rate ~–4 K/min in a heating mode over a wide temperature range from 100 K up to 300 K with steps of 5 - 10 K. To reach the thermal equilibrium, the sample was kept at a given temperature for 10 minutes before starting *three* spectra accumulations. The temperature stability was ± 0.5 K. The microwave power and the amplitude of the field modulation were optimized to avoid the signal distortion. The ESR spectra were evaluated in terms of the spectral parameter of mobility, $2A_{zz'}(T)$, i.e.,z-component of the anisotropic tensor of hyperfine interaction $A(T)$, corresponding to the outermost peaks separation of the triplet spectra of the *spin probe* of *nitroxide* type in a given *medium*, as a function of temperature and the subsequent determination of the spectral T_{50G} parameter [50,54]. This is the characteristic ESR temperature at which $2A_{zz'}$ reaches the conventional value of 50 Gauss (G). Furthermore, additional characteristic ESR temperatures can be obtained describing in detail the slow to fast regime transition

zone over more or less wide temperature interval around T_{50G} as well as in both slow and fast motion regimes: T_{Xi}^{slow}, T_{Xi}^{fast} [55–57]. In addition to this anisotropic hyperfine splittting parameter, $A_{zz'}$(100 K), the isotropic hyperfine constants, A_{iso}(RT) of the *spin probe TEMPO* as a measure of its interaction with a given *medium* were determined at room temperature under the fast motion condition in low-viscosity *media* [50].

4. Conclusions

The spectral and dynamic behaviours of the *spin probe TEMPO* in a series of *1-alkanols* ranging from *methanol* to *1-decanol* over a wide temperature range from 100 K up to 300 K using *electron spin resonance (ESR*) are reported. For all of *alkanols*, the main characteristic ESR temperatures connected with the slow to fast motion regime transition, namely, T_{50}'s and T_{X1}^{fast}'s are situated above the corresponding glass temperatures, T_g, and for the first five *shorter members* T_{50G}'s lie in the vicinity of melting point, T_m, while for the *longer ones* the $T_{50G} < T_m$ relationship indicates that the *TEMPO molecules* are in the local disordered regions of the *crystalline media*. The T_{X1}^{fast}'s are compared with the dynamic crossover temperatures, parametrized as $T_X^{VISC} = 8.72M^{0.66}$, as obtained by fitting the viscosity data in the liquid *n-alkanols* with the empirical power law. In particular, for N_C = 6-10 T_{X1}^{fast}'s lie rather relatively close to T_X^{VISC} as for *apolar n-alkanes*, while for N_C = 1-5 they are situated *above* the respective T_X^{VISC} in the vicinity of T_m. The absence of such a coincidence for lower *1-alkanols* indicates that the slow to fast motion transition is significantly influenced by the mutual interaction between the *polar TEMPO* and the *protic polar medium* due to the increased polarity and proticity which are destroyed at higher temperatures region connected to the larger-scale *solid*-to-*liquid* transition.

Author Contributions: Conceptualization,J.B.; methodology,J.B.; investigation,J.B. and H.Š.; analyses, J.B.and H. Š; data curation, J.B.; writing-original draft preparation, J.B.; writing-review and editing, J.B and H.Š.; visualization, J.B.; project administrationtion, J.B.

Funding: This research was funded by the VEGA, grant number 2/0005/20.

Institutional Review Board Statement: Not applicable.

Informed Consent Statement: Not applicable. Data Availability Statement: Not applicable.

Acknowledgments: The authors thank C. Corsaro for fruitful discussion.

Conflicts of Interest: The authors declare no conflict of interests.

References

1. Barlow, A.J.; Lamb, J.; Matheson, A.J. Viscous behavior of supercooled liquids. *Proc.Roy.Soc.London,Ser.A* **1966**, *292*, 322-342.
2. Taborek, P.; Kleinman, R.N.; Bishop, D.J. Power law behavior in the viscosity of supercooled liquids. *Phys.Rev.B*, **1986**, *34*, 1835-1840
3. Stickel, F.; Fischer, E.W.; Richert, R. Dynamics of glass-forming liquids. I. Temperature-derivative analysis of dielectric relaxation data. *J.Chem.Phys.* **1995**, *102*, 6251-6257.
4. Stickel, F.; Fischer, E.W.; Richert, R. Dynamics of glass-forming liquids. II. Detailed comparison of dielectric relaxation, dc-conductivity and viscosity data. *J.Chem.Phys.* **1996**, *104*, 2043-2055.
5. Martinez-Garcia, J.C.; Martinez-Garcia, J.; Rzoska, S.; Huellinger, J. The new insight into dynamic crossover in glass forming liquids from the apparent enthalpy analysis. *J.Chem.Phys.* **2012,** *137*, 064501-8.
6. a. Leon, L.; Ngai, K.L. Rapidity of the Change of the Kohlrausch Exponent of the α-Relaxation of Glass-Forming Liquids at T_B or T_β and Consequence. *J.Phys.Chem. B* **1999**, *103*, 4045-4051; b. Ngai, K.L.; Roland, C.M. Development of cooperativity in the local segmental dynamics of poly(vinylacetate): synergy of thermodynamics and intermolecular coupling. *Polymer* **2002,** *43*, 567-573.
7. Schönhals, A. Evidence for a universal crossover behavior of the dynamic glass transition. *Europhys. Lett.*, **2001**, *56*, 815-521.
8. a. Johari, G.P.; Goldstein, M. Viscous Liquids and the Glass Transition. II. Secondary Relaxations in Glasses of Rigid Molecules. *J. Chem.Phys*. **1970**, *53*, 2372-2388; b.Beiner, M.; Huth, H.; Schröter, K. Crossover region of dynamic glass transition: general trends and individual aspects, *J. Non-Cryst.Solids* **2001,** *279*, 126-135; c. Mallamace, F.; Corsaro, C.; Leone,N.; Villari, V.; Micali, N.; Chen, S.H. On the ergodicity of supercooled molecular glass-forming liquids at the dynamic arrest: ortho-terphenyl case. *Sci.Rep*. **2014**, *4*, 3747.

9. Mallamace, F.; Branca, C.; Corsaro, C.; Leone, N.; Spooren, J.; Chen, S.H.; Stanley,H.E. Transport properties of glass-forming liquids suggest that dynamic crossover temperature is as important as the glass transition temperature, *Proc.Natl.Acad.Sci.U.S.A.,* **2010**, *107,* 22457-22462.
10. a. Roland, C.M. Characteristic relaxation times and their invariance to thermodynamic conditions. *Soft Matter* **2008**,*4*,2316- 2322; b. Roland, C.M. Relaxation Phenomena in Vitrifying Polymers and Molecular Liquids. *Macromolecules* **2010**, *43,* 7875–7890.
11. *a*. Götze, W.; Sjögren, L. Relaxation processes in supercooled liquids, *Rep.Progr.Phys*., **1992,** *55,* 241-376; b. Götze, W. Recent tests of the mode-coupling theory for glassy dynamics. *J.Phys.-Cond.Matter*, **1999,** *11*, A1-A45; c. Götze, W. Complex Dynamics of Glass-Forming Liquids,:A mode coupling theory, Oxford Univ.Press, Oxford, 2009.
12. Novikov, V.N.; Sokolov, A.P. Universality of the dynamic crossover in glass-forming liquids: A ''magic'' relaxation time. *Phys. Rev.E,* **2003**, *67,* 031507.
13. 13.a. Hyde, P.D.; Evert, T.E.; Cicerone, M.T.; Ediger, M.D. Rotational motion of molecular probes in orto-terphenyl and cis-poly-isoprene, *J Non-Cryst.Solids* **1991**, *131-133*, 42-47; b. Ediger, M.D. Spatially Heterogeneous Dynamics in Supercooled liquids. *Annu. Rev.Phys.Chem*. **2000**, *51*, 99–128. 14 .a. Andreozzi, L.; Schinoy, A.D.; Giordano, M.; Leporini, D. A study of the Debye–Stokes–Einstein law in supercooled fluids J. Phys.-Cond.Matter 1996, 8, 9605–9608; b. Andreozzi, L.;Faetti, M.; Giordano, M. Fractional Debye-Stokes-Einstein law and scaling of the rotational relaxation in molecular glass formers: linear and non-linear ESR studies. Rec.Res.Devel.Phys.Chem. 2001, 5, 219-254; c. Andreozzi, L.; Faetti, M.; Giordano, M.; Zulli, F. Length Scales and Dynamics in the Reorientational Relaxation of Tracers in molecular and Polymeric Glass Formers via ESR. J.Phys.Chem.B 2010, 114, 12833-12839.
14. a. Bartoš, J.; Šauša, O.; Bandžuch, P.; Zrubcová, J.; Krištiak, J. Free volume factor in supercooled liquid dynamics .*J. Non-Cryst. Solids* **2002,** *307–310*, 417–425. b. Bartoš, J.; Šauša, O.; Krištiak, J.; Blochowicz, T.; Rössler, E. Free-volume microstructure of glycerol and its supercooled liquid-state dynamics. *J.Phys.-Cond.Matter* **2001**,*13,* 11473 –11484.
15. Bartoš, J.; Corsaro, C.; Mallamace, D.; Švajdlenková, H.; Lukešová, M. ESR evidence of the dynamic crossover in the supercooled liquid states of a series of solid n-alkanes, *Phys.Chem.Chem.Phys.* **2018**, *20,* 11145-11151.
16. Ramos, M.A.;Talon, .; Jimenez-Riobóo, R.J.; Vieira, S. Low-temperature specific heat of structural and orientational glasses of simple alcohols *J. Phys.-Cond.Matter* **2003**, *15,* S1007.
17. http://webbooknistgov/chemistry/
18. Illers,K.H. Innere Rotationen in Festkörpern aus hoch- und niedrigmolekularen organischen Molekülen, *Rheol. Acta* **1964**, *3,* 183-193.
19. a. Faucher, J.A.; Koleske, J.V. Glass Transitions of Organic Compounds. 1.Lower Aliphatic Alcohols, *Phys. Chem. Glasses* **1966**, *7,* 202-208; b. Koleske, J.V.; Faucher, J.A. Glass Transitions of Organic Compounds. 2.Linear Aliphatic Alcohols, *Phys.Chem. Glasses,* **1974**, *15,* 65-67.
20. Sugisaki, H.; Suga, H.; Seki, S. Calorimetric Study of the Glassy state.III. Novel Type Calorimeter for Study of Glassy State and heat Capacity of Glassy Methanol, *Bull.Chem.Soc.Jpn*. **1968**, *41,* 2586-2591.
21. Lesikar, A.V. On the self-association of the normal alcohols and the glass transition in alcohol-alcohol solutions, *J.Solut.Chem.* **1977**, *6,* 81-93
22. Carpenter, M.R.; Davis, D.B.; Matheson, A.J. Measurement of the Glass Transition Temperature of Simple Liquids, *J.Chem.Phys.* **1967**, *48,* 2451-2454.
23. Haida, O.; Suga, H.; Seki, S. Calorimetric study of the glassy state XII. Plural glass transition phenomena of ethanol, *J.Chem. Thermodyn.* **1977**, *9*, 1133-1148; b. Brand, R.; Lunkenheimer, P.; Schneider, U.; Loidl,A. Excess wing in the dielectric loss of glass-forming ethanol: A relaxation process *Phys.Rev. B* **2000,** *62*, 8878-8883.
24. Murthy,S.S.N. Experimental study of dielectric relaxation in supercooled alcohols and polyols, *Mol.Phys.* **1996**, *97,* 691-709.
25. Koleske, J.V.; Faucher, J.A. Glass Transitions of Organic Compounds. III. Cellulose Substrate Technique and Aliphatic Alcohols, *Polym.Engn.Sci.* **1979**, *19,* 716-721.
26. a. El Goresy,T.; Böhmer, B. Diluting the hydrogen bonds in viscous solutions of n-butanol with n-bromobutane: A dielectric study, *J.Chem. Phys.* **2008**, 28, 154520 ; b. Bartoš, J.; Šauša, O.; Vyroubalová, M.; Maťko, I. Švajdlenková,H. Confined effects on Structural isomers in the MCM-41-SIL Matrix as Seen by extrinsic probes via PALS and ESR" n-Butanol vs. tert-Butanol *J.Phys. Chem. C* **2021**, *125,* 15796-15811.
27. Hassaine, M.; Jimenez-Rioboo, R.J.; Ramos, M.A.; Sharapova, I.V.; Koroyluk, O.A.; Krivchikov, A.I. Thermal properties and Brillouin scattering study of glass, crystal and „glacial" state in n-butanol, *J.Chem.Phys.* **2009,** *131,* 174508.
28. Novikov, V.N.; Rössler, E.A. Correlation between glass transition temperature and molecular mass in non-polymeric and polymer glass formers, *Polymer* **2013**, *54,* 6987-699113.
29. Kauzmann, W. The nature of the glassy state and the behavior of liquids at low temperature, *Chem.Rev.* **1948,** *43*,219-256.

30. Boyer, R. The relation of transition temperatures to chemical structure in high polymers, *Rubber Chem.Technol.* **1963,** *36,* 1303-1421.
31. Sakka, S.; McKenzie,J.D. Relation between apparent glass transition temperature and liquidus temperature for inorganic glasses, *J. Non-Cryst. Solids* **1971**, 6, 145-162.
32. Landolt-Börnstein - Group IV Physical Chemistry, Pure Organic Liquids, Subvolume B 'Pure Organic Liquids' of Volume 18 Viscosity of Pure Organic Liquids and Binary Liquid Mixtures' of Landolt-Börnstein - Group IV Physical Chemistry.
33. R. Rowley, DIPPR Data Compilation of Pure Chemical Properties, Design Institute for Physical Properties, 2010 (Ref Type: Electronic Citation).
34. Barrera,M.C.; Jorge, M. A Polarization-Consistent Model for Alcohols to Predict Solvatation Free Energies, *J.Chem.Info & Modelling* , **2020**, *60,* 1352-1367.
35. Tamman, G.; Hesse, W.Z. Die Abhängigkeit der Viskosität von der Temperatur die unterkühlten Flüssigkeiten, *Zeitsch.Anorg. Allgem.Chem.* **1926**, *156,* 245-257.
36. Denney, D.J. Viscosities of some undercooled liquid alkylhalides, *J.Chem.Phys.* **1959**, *30,* 159-162.
37. Campbell Ling, A.A.C.; Willard, J.E. Viscosities of some organic glasses used as trapping matrixes, *J.Phys.Chem*. **1968**, *72,* 1918-1923.
38. Mitsukuri, S.; Tonomura, T. *Proc. Imper Academy of Japan* **1927**, *3,* 155 and **1929**, *5,* 23.
39. Krakoviack, V.; Alba-Simionesco, C.; Krauzman, M. Study of the depolarized light scattering spectra of supercooled liquids by a simple mode-coupling model, *J.Chem.Phys.*, **1997**, *107,* 3417-3427.
40. a.Bartoš, J.; Švajdlenková, H.; Šauša, O.; Lukešová, M.; Ehlers, D.; Michl, M.; Lunkenheimer, P.; Loidl,A. Molecular probe dynamics and free volume in organic glass-formers and their relationships to structural relaxation:1-propanol. *J.Phys.-Cond.Matt.*, **2016**, *28,* 015101.
41. Dodd, G.H.; Barratt, M.D.; Rayner, L. Spin probes for binding site polarity, *FEBS* **1970**, *8,* 286-288.
42. Jolicoeur, C.; Friedman, H.L. Hydrophobic nitroxide radicals as probes to investigate the hydrophobic interaction, *J.Sol. Chem.* **1974**, *3,* 15-43.
43. Al-Bala, R.D. Bates,Jr. R.D. Medium Effects on ESR Spectra in Studies of Hydrogen-Bonded Transient Solvent-Solute Complexes, *J.Magn.Res.* **1987**, *73,* 78-89.
44. Laleveé, J.; Allonas,X.; Jacques, P. Electronic distribution and solvatochromism of investigation a model radical 2,2,6,6-tetramethyl piperidine N – oxyl: TEMPO through TD-DFT calculation including PCM solvatation, *J.Mol.Struct.Theochem.* **2006**, *767*,143-147.
45. Kawamura, T.; Matsunami, S.;Yonezawa, T. Solvent Effects on the g-value of Di-t-butyl Nitric oxide, *Bull.Chem.Soc.Jpn.* **1967**, *40,* 1111-1115.
46. Griffith, O.H.; Dehlinger, P.J.; Van, S.P. Shape of the Hydrophobic Barrier of Phospholipid Bilayers (Evidence for Water Penetration in Biological Membranes), *J.Membrane Biol.* **1974**, *15,* 159-192.
47. Krinichnyi, V.I.; Grinberg, O.Y., Bogatyrenko, V.R.; Likhtenshtein, G.I.; Lebedev, Ya.S. *Biophysics* **1985,** *30,* 233.
48. Ondar, M.A.; Grinberg, O.Y.; Dubinskii,A.A.; Lebedev, Ya.S. *Sov.J.Chem.Phys.* **1985**, *3*, 781.
49. Owenius, R.; Engström, M.R.; Lindgren, M. Influence of Solventr Polarity and Hydrogen Bonding on the EPR parameters of a Nitroxide Spin label Studied by 9-GHZ and 95-GHz EPR Spectroscopy and DFT calculations, *J.Phys.Chem*. **2001**, *105*, 10967-10977.
50. Seelig, J.; Limacher, H.; Bader, P. Molecular Architecture of Liquid Crystalline Bilayer, *J.Amer.Chem Soc.* **1972,** *94,* 6364-6371.
51. L.Onsanger, Electric Moments of Molecules in Liquids, *J.Amer.Chem.Soc.* **1936**, *58,* 1486-1493.
52. Böttcher,C.J.F. *Theory of Electric Polarisation*, Elsevier, New York, N. Y., Amsterdam, 1952, pp. 70.
53. Rabold, G.P. Spin-Probe Studies.II. Applications to Polymer Characterization, *J.Polym.Sci. A,* **1969**, *7,* 1203-1223.
54. Bartoš, J.; Švajdlenková, H.; Zaleski, R.; Edelmann, M.; Lukešová, M. Spin probe dynamics in relation to free volume in crystalline organics by means of ESR and PALS: n-Hexadecane, *Physica B Cond.Mat.*, **2013**, ***430***, 99-105.
55. Švajdlenková, H.; Iskrová, M.; Šauša, O.; Dlubek, G.; Krištiak, J.; Bartoš, J. The Spin probe Dynamics and the Free Volume in a series of Amorphous Polymer Glass-Formers, *Macromol.Symp.*, **2011**, *305,* 108-115.
56. Švajdlenková, H.; Arrese-Igor, S.; Nógellová, Z.; Alegría, A.; Bartoš, J. Molecular dynamic heterogeneity in relation to free volume and relaxation dynamics in organic glass-formers: oligomeric cis-1,4-poly(isoprene), *Phys.Chem.Chem.Phys.*, **2017**, *19*, 15215-15226.